Osborne Anne, Helen (Orcid ID: 0000-0003-3195-8855)

Hathorne Ed (Orcid ID: 0000-0002-7813-2455)

Groeneveld Jeroen (Orcid ID: 0000-0002-8382-8019)

Late Pliocene and Early Pleistocene variability of the REE and Nd isotope composition of Caribbean bottom water: A record of changes in sea level and terrestrial inputs during the final stages of Central American Seaway closure

Anne H. Osborne[1]*, Ed C. Hathorne[1], Philipp Böning[2], Jeroen Groeneveld[3], Katharina Pahnke[2], and Martin Frank[1]

[1]GEOMAR Helmholtz Centre for Ocean Research Kiel, Germany. [2]Institute for Chemistry and Biology of the Marine Environment (ICBM), University of Oldenburg, Oldenburg, Germany. [3]Alfred Wegener Institute, Helmholtz Centre for Polar and Marine Research, Potsdam, Germany.

*Corresponding author: Anne H. Osborne (aosborne@geomar.de)

Key Points:

- REEs can be used to identify local influences on the Nd isotope record in the deep Caribbean
- Distinct terrestrial REE signal in the deep Caribbean associated with Late Pliocene and Pleistocene closure events of the Central American Seaway
- Ce/Ce* records a ventilation signal despite input of terrestrial material.

This article has been accepted for publication and undergone full peer review but has not been through the copyediting, typesetting, pagination and proofreading process which may lead to differences between this version and the Version of Record. Please cite this article as doi: 10.1029/2019PA003654

Abstract

The isotopic composition of neodymium dissolved in seawater consists of a distal, advected component that reflects water mass mixing and circulation, but near land can also contain a large local component originating from terrestrial sources such as aeolian or fluvial material. In order to use Nd isotopes to reconstruct paleocirculation, it is important to detect any local influences on the seawater signal recorded in deep sea sediments. Here we present rare earth element (REE) and Nd isotope (ε_{Nd}) records from the deep Caribbean for two well-studied time intervals in the Late Pliocene and Early Pleistocene. We measured trace element and REE compositions of weakly cleaned foraminifera to investigate if the Nd isotope signal from the same samples contained a local component. We find distinct changes in REE compositions across glaciations that are consistent with increases in the supply of local terrestrial material to the basin likely the results of glacially driven changes in sea level. Despite these larger terrestrial inputs, the Ce anomaly (Ce/Ce*) became more pronounced during glaciations indicating a better deep Caribbean ventilation. Short negative Nd isotope excursions occurred during three of the four studied glaciations, independently of any other proxy indicators for changes in ocean circulation suggesting that inputs from local terrigenous sources of Nd controlled the signal. We recommend that studies that aim to use ε_{Nd} as a paleocirculation tracer routinely measure REE compositions of the authigenic phase to identify any possible terrestrial influence on the signal.

1. Introduction

The $^{143}Nd/^{144}Nd$ ratio of dissolved Nd in seawater (usually reported as ε_{Nd}, the parts per ten thousand deviation of the measured $^{143}Nd/^{144}Nd$ from that of the chondritic uniform reservoir (CHUR) of 0.512638, *Jacobsen & Wasserburg*, 1980) has been used extensively as a tracer for the advection of past water masses and their mixing (e.g. *Burton et al.*, 1997*; Gutjahr et al.*, 2008; *Roberts et al.*, 2010*; Scher & Martin*, 2006). However, recent publications have called into question the robustness of this approach in light of evidence for a benthic sedimentary source of Nd to bottom waters (Abbott et al., 2015a,b; 2016; 2019) and modification of the seawater ε_{Nd} signal not just near to continental boundaries (e.g. *Grenier et al.*, 2013; *Jeandel et al.*, 1998, 2007; *Lacan & Jeandel*, 2001, 2004a, 2004b, 2004c, 2005a, 2005b; Wilson et al., 2012; Abbot 2019) but potentially throughout the ocean (Haley et al., 2017; Abbott 2019; Abbott et al., 2019). Point sources of terrestrial material to the oceans, such as river estuaries, can also have a far-reaching impact on the ε_{Nd} signal. For example, *Bayon et al.* (2004) found that pre-formed riverine oxides from the Congo River dominated the ε_{Nd} signal in sediment coatings from a core 1000 km to the south of the river mouth, and *Stewart et al.* (2016) found that partial dissolution of detrital particulate material from the Amazon exerted a strong control on the ε_{Nd} record from the Ceara Rise, approximately 800 km from the river mouth.

This raises the question if the authigenic ε_{Nd}-signal in the sediment record can only be used as a water mass circulation tracer in the open ocean where possible contributions from terrestrial material do not modify the bottom water signal. Can other proxies be used in combination with ε_{Nd} to assess whether or not it is a robust circulation tracer at a particular location?

Weakly cleaned planktonic foraminifera (i.e. only cleaned to remove salts and detrital particles) have been demonstrated to reliably record the ε_{Nd} signature of ambient bottom waters (*Roberts et al.*, 2010; *Piotrowski et al.*, 2012; *Huang et al.*, 2014), although it is not

known whether the Nd is present predominantly in post depositional "coatings" or incorporated into the crystal lattice of the foraminifera during early diagenesis (*Bayon et al.,* 2004; *Roberts et al.,* 2012; *Tachikawa et al.,* 2014; *Skinner et al.,* 2019; *Abbott et al.,* 2019). Simply comparing core-top compositions with bottom water ε_{Nd} cannot distinguish between a benthic source and a circulation source of Nd (*Abbott et al.,* 2016; 2019). Trace element ratios, such as Al//Nd, are routinely used as a test for detrital contributions to the measured ε_{Nd} signal (*Hein et al.,* 1999; *Gutjahr et al.,* 2007) but Nd added to pore waters, for example via dissolution of clays, would not necessarily result in a detrital-like composition of the leachable fraction (*Abbott et al.* 2019). Seawater-like Rare Earth Element (REE) patterns in the authigenic component have also been used as an indicator for the recovery of the seawater signal (e.g. *Gutjahr et al.,* 2007; *Blaser et al.,* 2016). Such patterns could, however, also be mimicked by the preferential uptake of the light REEs (LREEs, La to Sm) by authigenic clay minerals resulting in an enrichment in heavy REEs (HREEs, Ho to Lu) in the pore waters from which the REEs precipitate (*Abbott et al.,* 2019). In conclusion, there is at present no simple test to reliably identify or quantify the origin of 'authigenic' Nd in deep sea sediments.

Here we apply a multi-proxy approach to examine the controls on the ε_{Nd} extracted from weakly cleaned planktonic foraminifera in Plio-Pleistocene sediments from the deep Caribbean basin (ODP Site 999). This site was chosen because it shows distinct changes in both bottom water and surface water properties affected by episodic closure of the Central American Seaway (CAS) during glacial-interglacial cycles in the Late Pliocene (MIS M2; ~3.3 Ma) (*De Schepper et al.,* 2013; *Haug and Tiedemann,* 1998) and the early Pleistocene (MIS 95-100; ~2.5 Ma) (*Groeneveld et al.,* 2014). Site 999 is 400 km from the mouth of the Magdalena River, which discharges approximately 150 MT/yr of sediment into the Caribbean Sea, putting it in the top ten of world river sediment loads (*Restrepo et al.,* 2006). As a result, climatically driven changes in the input of terrestrial-derived sediments may also be expected. We measured ε_{Nd} in weakly cleaned foraminifera and use the REE compositions measured on the same samples to assess whether the ε_{Nd} signal recorded a water mass circulation signal or whether it was predominantly controlled by local terrestrial sources.

2. Materials and Methods

2.1. Sample site and oceanographic setting

ODP Site 999 (12º45'N, 78º44'W) was drilled at 2828 m water depth on the Kogi Rise in the Columbian basin, approximately 400 km to the northwest of the Magdalena River mouth. Samples were taken from the upper 150 m of the core, which consists of mixed nannofossil, foraminifera and clay sediments and between 5 and 20 % dispersed volcanic ash (*Sigurdsson et al., 1997*). Nepheloid clays and other fine-grained terrigenous material from the Magdalena submarine fan have been deposited on the Kogi Rise but the elevated position of Site 999 above the Colombian Plain has protected it from the influence of turbidites that dominate sedimentation to the southeast (*Sigurdsson et al., 1997*).

The Anegada-Jungfern sill (~ 1800 mbsl) is the deepest connection between the Caribbean and the Atlantic and is the only pathway for overflow into the abyssal Columbian basin (*Johns et al.,* 2002). The water filling the Caribbean below ~ 1800 m water depth is predominantly UNADW (*Wüst,* 1964) with small contributions from AAIW (10 %) and Mediterranean Outflow Water (MOW, 5%) (*deMenocal et al.,* 1992; *Kawase & Sarmiento,* 1986). Deep water remains in the Caribbean basin for an average of ~150 years (*Joyce et al.,* 1999) before exiting via the same sill (*Sturges,* 2005). Prolonged interaction with sediments in the basin, such as those from the Magdalena River (ε_{Nd} = -8.3, *Goldstein et al.,* 1984) or

from the Caribbean islands and Central American Volcanic Arc (*Kirillova et al.*, 2019; *GEOROC database*) is likely responsible for the moderately radiogenic (i.e. higher $^{143}Nd/^{144}$ Nd ratio and more positive ε_{Nd} value) isotope composition of dissolved Nd in the deep Caribbean (ε_{Nd} signal between -8.3 and -9.2) (*Osborne et al.*, 2014b), which is at least 4 ε_{Nd} units more radiogenic than the signal of the inflowing Atlantic waters (-13 ε_{Nd}, *deMenocal et al.*, 1992; *Kawase & Sarmiento*, 1986; *Piepgras & Wasserburg*, 1987; *Tachikawa et al.*, 2004).

2.2. Age models

The original age model for ODP Site 999 (*Haug & Tiedemann*, 1998) was updated by *Steph et al*. (2006) and specifically tuned to LR04 (*Lisiecki & Raymo*, 2005) for MIS M2 by *De Schepper et al.* (2013) and for MIS 95-100 by *Groeneveld et al*. (2014).

2.3. Sample preparation

Samples of between 40 and 120 mg of mixed planktonic foraminifera were picked from the > 400 µm size fraction for MIS 95-100 and from the > 355 µm size fraction for MIS M2 and cracked between two glass plates to open all chambers. Clays were removed by ultrasonication in repeated rinses of distilled water and methanol (*Boyle*, 1981). Any remaining detrital particles found under the microscope were removed with a single paintbrush bristle before the samples were dissolved in 0.03 M HNO_3. We refer to the foraminifera prepared in this way as having been 'weakly cleaned' (cf. *Skinner et al.*, 2019). Ten percent of the solution was retained for trace element and YREE-U measurements (REE plus yttrium and uranium). The neodymium in the remaining solution was separated and purified using standard ion chromatographic procedures (cation exchange columns, 0.8 ml AG50W-X12, mesh 200-400 µm, *Barrat et al.*, 1996; 2 ml Ln Spec resin, mesh 50-100 µm, *Le Fèvre and Pin*, 2005).

2.4. Nd isotope analyses

The Nd isotope compositions were measured on a Neptune Plus at the Max Planck Research Group for Marine Isotope Geochemistry at ICBM, University Oldenburg. Measured $^{143}Nd/^{144}Nd$ ratios were mass bias corrected using a $^{146}Nd/^{144}Nd$ ratio of 0.7219 and the exponential law and were normalized to the accepted JNdi-1 standard $^{143}Nd/^{144}Nd$ ratio of 0.512115 (*Tanaka et al.*, 2000). The external reproducibility for Nd isotope analyses was determined by replicate measurements of JNdi-1 and was ± 0.000015 for $^{143}Nd/^{144}Nd$ (± 0.30 ε_{Nd}; n = 38; 2σ). Repeated measurements of the La Jolla standard gave 0.511860 ± 0.000012 (2SD, n=7), consistent with the reported value of 0.511858 (*Lugmair et al.*, 1983). Internal precision was between 9 and 23 ppm (2SE). Total procedural blanks were ≤ 50 pg Nd, equivalent to ≤ 0.2 % of the total sample and thus considered negligible. Results and reproducibilities are reported in Supplementary Table 1. All ε_{Nd} values were corrected for the ingrowth of ^{143}Nd from ^{147}Sm (0.02 ε_{Nd} units for all samples) using an average Sm/Nd ratio of 0.139 for weakly cleaned foraminifera (*Osborne et al.*, 2017).

2.5. Trace and Rare Earth Element analyses

Concentrations of Ca, Fe, Mn, Al, La and Nd were measured on an Agilent 7500ce ICP-MS at GEOMAR. Standards with element/Ca ratios similar to foraminifera were prepared from single element solutions and were used to calculate the element/Ca ratios of the samples (*Kraft et al.*, 2013; *Rosenthal et al.*, 1999). External reproducibilities were monitored using repeat measurements of the ECRM standard (*Greaves et al.*, 2008) and were 19.9% for Al/Ca, 2.1 % for Mn/Ca, 4.5 % for Fe/Ca, 25.7% for Al/Nd and 5.3 % for Fe/Mn. Results are

reported in Supplementary Table 2. All samples were then diluted to 50 ppm Ca and REE, Y and U concentrations (hereafter referred to as YREE-U) were determined using a seaFAST online pre-concentration system (Elemental Scientific Inc., Nebraska, USA) attached to the same Agilent 7500ce ICP-MS. Measurement procedures were modified from *Hathorne et al.* (2012) by inclusion of Y and U and of a time resolved analysis of the elution peak, which improved analytical precision (*Osborne et al.,* 2015; 2017). The La/Ca ratio (µmol/mol) measured by standard introduction was used to normalize YREE-U concentrations. External reproducibilities for both were monitored using repeat measurements of the ECRM standard (*Greaves et al.,* 2008) and were between 5 and 9 % for YREE-U. Results and procedural blanks are reported in Supplementary Table 3.

3. Results

3.1. ε_{Nd}

The deep Caribbean $\varepsilon_{Nd(t)}$ signal extracted from the weakly cleaned planktonic foraminifera shells for the Late Pliocene time interval investigated varied by 2 ε_{Nd} units between -5.9 for the oldest sample (3.344 Ma) and -7.9 at the beginning of the MIS M2 glaciation (3.311 Ma) (Figure 2a). Radiogenic ε_{Nd} peaks reaching values between -6.0 and -6.5 were recorded during both interglacial MG1 and glacial M2. The ε_{Nd} signal remained at ~ -7 from 3.297 Ma until the end of our record at 3.260 Ma.

The early Pleistocene ε_{Nd} signatures varied between -6.5 and -8 (Figure 3a) and thus were overall only slightly less radiogenic than the Late Pliocene record (Figure 2a). Again, there were radiogenic ε_{Nd} peaks during both glacials and interglacials. A sudden drop to an ε_{Nd} signal of ~ -8.0 was recorded in the middle of the MIS 98 glaciation (2.487 Ma) and at the beginning of the MIS 96 glaciation (2.453 Ma).

3.2. Trace and Rare Earth Element composition

Concentrations of the redox sensitive elements U, Mn and Fe were determined for the same weakly cleaned foraminifera samples (Supplementary Tables 2 and 3). Uranium concentrations decreased from 0.4 ppm at 3.344 Ma to between 0.1 and 0.2 ppm after 3.322 Ma, with a peak of 0.6 ppm at 3.323 Ma (Figure 2b). Mn concentrations fluctuated between 600 and 900 pm throughout the Late Pliocene record (Figure 2c). Fe concentrations were between 150 and 400 ppm for the majority of the Late Pliocene record, with higher concentrations (> 500 ppm) prior to 3.336 Ma and a peak of ~ 1000 ppm at 3.323 Ma (Figure 2d), concurrent with the peak in U. Concentrations of Nd were highest during the first half of the M2 glaciation (between 1.7 and 2.6 ppm from 3.311 and 3.288 Ma) (Figure 2e), a trend observed for all REEs (Figure 4a).

In the early Pleistocene record, U concentrations were highest during interglacials 95 and 97 (> 0.4 ppm at 2.463 Ma) and lowest during glaciations 98 and 100 (< 0.1 ppm) (Figure 3b). Mn concentrations fluctuated between 300 and 900 ppm (Figure 3c). Fe concentrations were mostly between 100 and 500 ppm, with a small peak of 760 ppm at 2.499 Ma and a larger peak of 1700 ppm at 2.463 Ma (Figure 3d). Nd concentrations were highest at the start of glaciations (reaching a maximum of 3.0 ppm at 2.529 Ma), decreasing during the glaciations to minima during the interglacials (approaching minimum values near 1 ppm) (Figure 3e). The concentrations of all REEs were generally higher during the glaciations (Figure 4b).

4. Discussion

4.1. Evidence for an authigenic, seawater-derived ε_{Nd} signal

The Al/Nd ratio is often applied as an indicator of detrital contamination as it is generally significantly lower in ferromanganese coatings than in detrital sediments (*Hein et al.,* 1999; *Gutjahr et al.,* 2007). The range of Al/Nd elemental ratios determined for the weakly cleaned foraminifera is between 2 and 37 for both time slices, with a mean of 8.4 for MIS M2 and 10.1 for MIS 95-100, which is comparable to the first 3-hour leach in *Gutjahr et al.* (2007). The overall small changes in Al/Nd do not coincide with any of the prominent changes in the ε_{Nd} and REE records (Figures 2f and 3f). Based on these observations we argue that the ε_{Nd} signature extracted from the weakly cleaned foraminifera was not contaminated by detrital particles. However, as *Abbott et al.* (2019) pointed out, the dissolution and re-precipitation of authigenic clays would not necessarily result in a high Al/Nd ratio, and neither would a preformed fluvial signal transported from local rivers [*Bayon et al.,* 2004; *Stewart et al.,* 2016]. Therefore Al/Nd ratios alone cannot distinguish between a circulation or local source of Nd in the records.

Looking now at the ε_{Nd} signal obtained from the weakly cleaned foraminifera, both records have a similar range in compositions, with minima at -8.0 ε_{Nd} and maxima between -6.5 and -6.0 ε_{Nd} (Figures 2a and 3a). The minima are similar to the composition of core top foraminifera from close to Site 999 (-8.1 to -9.3 $\varepsilon_{Nd,}$ *Osborne et al.,* 2014a) and to modern deep waters in the Caribbean (ε_{Nd} signal between -8.3 and -9.2, *Osborne et al.,* 2014b). The minima are also similar to the composition of Magdalena River sediments (ε_{Nd} = -8.3, *Goldstein et al.,* 1984). The remainder of the Late Pliocene and Early Pleistocene records require a different composition of incoming Atlantic waters compared to the modern situation and/or a change in the local supply of Nd to the basin.

The Pliocene composition of NADW, as recorded by a NW Atlantic ferromanganese crust at 1850 m water depth, was ~ -11.35 ε_{Nd} at 3.33 Ma, decreasing slightly to ~ -11.55 ε_{Nd} at 2.5 Ma (*Burton et al.,* 1999). The composition of AAIW was -6 ± 0.5 ε_{Nd} during the Late Pliocene and Early Pleistocene (*Karas et al., 2019*) and MOW ε_{Nd} was between -11 and -10 (*Khelifi et al.,* 2014). If the contribution of radiogenic Nd from local sources was similar to today (+ 4 ε_{Nd} *Osborne et al.,* 2014b) then an increase in the proportion of AAIW in the deep Caribbean of up to 25 ± 10 % compared to 10 % today (*deMenocal et al.,* 1992; *Kawase & Sarmiento,* 1986) could explain the most radiogenic signals of the Site 999 record. However, a constant contribution of + 4 ε_{Nd} cannot explain compositions less radiogenic than ~ - 7.35 ε_{Nd}, even if 100 % NADW filled the basin at those times. Therefore, there must have been a change in the contribution of Nd from local sources which dominated the observed signatures but was likely accompanied by a change in water mass mixing.

The other possible factors contributing to the ε_{Nd} signal were a change in the composition of Magdalena river sediments transported to the site or an increase in the deposition of volcanic ash.
The Magdalena River Basin today covers more than 250,000 km^2, and is a tectonically active area with steep hill slopes (*Restrepo et al.,* 2006). The river and its tributaries drain the Western, Central and Eastern Cordillera, which together comprise the northernmost part of the Andean mountain chain (*Restrepo et al.,* 2006). Sediments from the continental and metamorphic basement in the Eastern and Central Cordillera have very unradiogenic compositions, ($\varepsilon_{Nd} \leq$ -13) whereas those with a magmatic arc source in the Western Cordillera

are more radiogenic (-12 to -9 ε_{Nd}) (*Nie et al.,* 2012). Jurassic plutonic and volcanic units in the Colombian Andes are generally more radiogenic than the basement complexes, ranging from -10.3 to +4.0 ε_{Nd} (*James and Murcia.,* 1984; *Quandt et al.,* 2018). Therefore, a preformed signal transported by sediments from the Magdalena river could explain the full range of ε_{Nd} values in our Plio-Pleistocene records. *Sigurdsson et al.* (1997) reported that material from the upper 150 m of ODP 999 contained between 5 and 20 % of dispersed volcanic ash. There is no available record of ash content that has the same temporal resolution as the records presented here but it is conceivable that variations did occur and contributed to the ε_{Nd} signal recorded by the weakly cleaned foraminifera.

4.2. **Glacial-interglacial changes in REE compositions**

The REE results show clear glacial-interglacial differences, with higher concentrations during glaciations of both studied time intervals (Figures 2e, 3e, 4a and 4b). Glacial samples tend to have a more pronounced Middle REE enrichment and a greater reduction in Ce concentration compared to La and Pr, whereas interglacial samples are generally more enriched in the Heavy REE than in the Light REEs (Figure 4).

The first question to ask is whether these shifts in REE compositions were a result of changing redox conditions in the sediment column. If sub-oxic or anoxic conditions prevail during early diagenesis this can strongly alter the REE composition of the porewaters (*Abbott et al.,* 2015; *Elderfield & Sholkovitz,* 1987; *Haley et al.,* 2004; *Holser,* 1997; *Sholkovitz et al.,* 1992) and can overprint the primary core-top REE signal (*Du et al.,* 2016*; Skinner et al.,* 2019). Uranium is soluble under oxic conditions and under anoxic conditions precipitates onto sedimentary particles and foraminifera (*Henderson & O'Nions,* 1995; *Lea et al.,* 2005; *Boiteau et al.,* 2012). Uranium concentrations are low in the down core foraminifera samples (< 0.6 ppm), supporting oxic conditions during deposition and burial, but Fe concentrations in our records (≥ 150 ppm, Figures 2b and 3b) are significantly higher than concentrations of sedimentary foraminifera reported by *Roberts et al.* (2012) (≤ 50 ppm), and manganese concentrations (360 – 900 ppm, Figures 2c and 3c) are comparable with the glacial sections of the *Roberts et al.* (2012) record, which was inferred to have been deposited under sub-oxic conditions. However, there are multiple peaks in Mn concentrations during both time intervals which do not follow glacial-interglacial patterns and do not correlate with the peaks in Fe, which argues against pervasive re-dissolution and re-precipitation of oxides that would be expected for systematic changes between reducing and oxidizing conditions (*Froelich et al.,* 1979) (Figures 2 and 3). Furthermore, neither Mn nor Fe concentrations are tightly coupled with Nd concentrations in our records, despite the strong affinity of Nd (and the other REEs) to ferromanganese oxides (*Koschinsky & Hein,* 2003). This argues against dissolution and re-precipitation of Fe-Mn-oxides under changing redox conditions being responsible for the observed shifts in REE concentrations (*Roberts et al.,* 2012) (Figures 2 and 3).

The ratio of heavy to light REEs (HREE/LREE, defined as $[Yb_N + Lu_N]/[Pr_N + Nd_N]$), the Middle REE enrichment (MREE/MREE*, defined as $2[Tb_N + Dy_N]/[Pr_N + Nd_N + Yb_N + Lu_N]$, and the Ce/Ce* anomaly ($3*Ce_N/(2*La_N+Nd_N)$ (*Elderfield & Greaves,* 1982), all show distinct and systematic glacial-interglacial changes that are independent of the proxies for redox conditions (In all cases $_N$ is normalisation to Post-Archaean Australian Shale (PAAS, *Taylor & McLennan,* 1985) (Figures 2g-i and 3g-i).

The differences between concentrations of dissolved REEs are largely dependent on different mineral-seawater partitioning coefficients (*Byrne & Kim,* 1990; *Schijf et al.*, 2015). LREEs are more readily scavenged than HREEs (*Byrne & Kim,* 1990; *Schijf et al.* 2015), leading to a general increase of the HREE/LREE ratio in a water mass the longer it is isolated from continental REE inputs (cf. *Osborne et al.*, 2017). An enrichment of the MREEs (Eu to Dy) relative to the Heavy and Light REEs in seawater indicates that a water mass recently received input from terrestrial (i.e. dust or river) REE sources (e.g. *Freslon et al.*, 2014; *Osborne et al.*, 2017; *Pourmand et al.,* 2014; *Sholkovitz*, 1993).

The simplest explanation for the increase in REE concentrations, as well as the enrichment in the MREEs and HREE/LREE ratios trending towards 1, is an increase in inputs from terrestrial REE sources during glacial periods (e.g. *Freslon et al.*, 2014; *Osborne et al.*, 2017; *Pourmand et al.*, 2014; *Sholkovitz*, 1993). However, increased terrestrial input should also shift the Ce/Ce* anomaly towards 1 (*German & Elderfield,* 1990; *Hathorne et al*., 2015) but instead the opposite trend is observed. Cerium differs from the other REEs in that Ce(III) oxidises to insoluble Ce(IV) and is preferentially removed from oxygenated seawater in comparison to the other REEs and is re-released under reducing conditions (*Elderfield & Sholkovitz, 1987*). There are indications that lower oxygen concentrations in bottom waters correspond to a greater "Ce-enrichment" in sedimentary foraminifera compared to the overlying seawater (*Skinner et al.*, 2019). Taking these observations into account, we suggest that the enhancement of the Ce/Ce* anomaly during the glaciations was independent of increased terrestrial input and was instead the result of better-oxygenated bottom- and pore-waters. This conclusion is supported by concomitant increases in the percentage of carbonate sand that have been interpreted as maxima of deep Caribbean ventilation (*Haug & Tiedemann*, 1998).

4.3. Multi-proxy assessment of the origin of the ε_{Nd} changes

We now combine the REE results with the ε_{Nd} records and compare these to other proxies from Site 999 in order to examine the origin of the ε_{Nd} signal.

There is a striking similarity between the ε_{Nd} and the HREE/LREE records up until the onset of MIS M2 (Figure 5b and c). Both show a maximum during MIS MG1 followed by a decrease at the boundary to MIS M2. The Pliocene MREE/MREE* record (Figure 5d) is generally anti-correlated with the HREE/LREE and ε_{Nd} records and we therefore interpret the more radiogenic ε_{Nd} values during MIS MG1 as a circulation signal, implying a greater proportion of AAIW in the waters that enter the Caribbean and sink to form deep water. Low carbonate sand percentages (*Haug & Tiedemann,* 1998) and a weak Ce/Ce* anomaly during this interval support the presence of poorly ventilated waters in the Caribbean basin (Figures 2f and g).

Both the HREE/LREE ratio and the ε_{Nd} signature decrease at the boundary to MIS M2. As discussed above, elevated inputs of terrestrial REEs close to the sample site would push the HREE/LREE towards 1. As the ε_{Nd} minimum is similar in composition to modern Magdalena River Sediments (Figure 5b) (*Goldstein et al.* 1984), one viable interpretation is that there was an increase in sediment discharge from that river at the onset of MIS M2. If this was the case, then we would also expect to see an increase in the MREE/MREE* enrichment that is typical of terrestrial REE sources (e.g. *Freslon et al.*, 2014; *Osborne et al.*, 2017; *Pourmand et al.*, 2014; *Sholkovitz*, 1993). Instead we see a minimum in

MREE/MREE* at the same time as the minimum in ε_{Nd} and HREE/LREE (Figure 5). The carbonate sand percentage is low at the MIS M2 boundary, suggesting the continued presence of poorly ventilated waters (*Haug & Tiedemann,* 1998), whereas the Ce/Ce* anomaly is stronger, which would suggest an increase in ventilation at the MIS M2 boundary. Based on the available data, the cause of the ε_{Nd} minimum at 3.311 Ma is therefore unclear at present.

During the most intense period of the MIS M2 glaciation (3.305-3.285 Ma) HREE/LREE ratios were lower and the MREE/MREE* enrichment was greater, both of which point to an increase in local terrestrial input. The carbonate sand percentage (*Haug & Tiedemann,* 1998) and Ce/Ce* anomaly records are also consistent with each other and indicate that the deep Caribbean was well-ventilated, an interpretation supported by higher benthic $\delta^{13}C$ during MIS M2 (*Haug & Tiedemann*, 1998; *De Schepper et al.*, 2013). The ε_{Nd} signal during MIS M2 increased to ~ -6.2 at 3.302 Ma before decreasing to ~ -7 after 3.294 Ma. These changes were independent of fluctuations in the REE composition. Based on the Pliocene record of NADW composition in the NW Atlantic (~ -11.35 ε_{Nd} at 3.33 Ma, *Burton et al.*, 1999), an increase in well-ventilated, northerly sourced waters would contribute unradiogenic Nd to the Caribbean basin, i.e. opposite to the observed trend. Therefore, we conclude that increased local inputs of radiogenic terrestrial material to Site 999 contributed to the signal at Site 999 during the glaciation.

Sea-level reconstructions vary widely for MIS M2, from >-10 m (*Naish and Wilson,* 2009) to -65 m ± 15-25 m (*Dwyer and Chandler*, 2009) (Figure 5g). An independent indicator for a sea-level low stand in the Caribbean during M2 comes from lower abundances of dinoflagellates, thought to be the result of a glaciation-induced closure of the Central American Seaway (Figure 5a, *De Schepper et al.*, 2013). Lower sea level would have exposed shallow shelf areas and promoted river incision, which would have increased the terrestrial input to the Caribbean. A further consideration is a shift in the precipitation regime associated with the glaciation. To our knowledge, there are no proxy records of precipitation in the Caribbean region for M2. Simulations of M2 conditions with a coupled atmosphere-ocean climate model show a southward shift of the ITCZ and a decrease in mean annual precipitation in the tropics (*Dolan et al.*, 2015), which would have reduced runoff via the Magdalena and other local rivers. Sediment records from the Cariaco Basin and the eastern equatorial Pacific also suggest drier conditions during the Younger Dryas and during glacials over the past 500 thousand years respectively (*Haug et al.*, 2001; *Rincon-Martinez et al.* 2010). More arid conditions during MIS M2 may have instead increased the supply of dust to the region. As both dust and river REEs show an MREE enrichment (*Freslon et al.*, 2014; *Pourmand et al.*, 2014; *Sholkovitz*, 1993) it is not possible at present to distinguish between these two potential source contributions.

The Pleistocene ε_{Nd} record shows a smaller amplitude than the Pliocene record, with the maximum ε_{Nd} values reduced from -6.0 to -6.5. Similar to the Pliocene record, the two ε_{Nd} minima in the Pleistocene record are also ~ -8.0 and occur in the middle of MIS 98 (2.487 Ma) and at the boundary between MIS 97 and 96 (2.453 Ma), at the same time as low HREE/LREE and high MREE/MREE* ratios. In this instance, all three proxies are consistent with increased contributions from a terrestrial REE source with a Magdalena River-like composition. The HREE/LREE and MREE/MREE* in the Pleistocene record closely track one another and co-vary with the ε_{Nd} signal during MIS 98 and 97 but not during the rest of the record. The HREE/LREE and MREE/MREE* ratios do, however, show a striking similarity to the mixed layer temperature difference measured between the Eastern Equatorial Pacific ODP Site 1241 and Site 999 (*Groeneveld et al.*, 2014). The mixed layer temperature

difference has been interpreted as a record of periodic Central American Seaway closure related to ice-volume driven drops in sea-level of up to 60 m (*Groeneveld et al.,* 2014; *Bintanja & van de Wal,* 2008). As for the Pliocene record, lower sea-level during the Early Pleistocene corresponded to a more terrestrial-like signal in the HREE/LREE and MREE/MREE* ratios.

The Pleistocene Ce/Ce* anomalies were more pronounced during the glacials and weakened during the interglacials, which does not correlate with any of the other REE parameters discussed here but broadly corresponds to changes in the carbonate sand percentage (*Haug & Tiedemann,* 1998). Together the data suggest, as for MIS M2, that the deep Caribbean was better ventilated during the glacials. Increases in benthic $\delta^{13}C$ during MIS 100 and 96 also support this interpretation (*Haug & Tiedemann,* 1998).

Apart from the two minima, the ε_{Nd} signal recorded at Site 999 was -7.0 ± 0.5 and does not show changes that are consistent with the proxies for terrestrial input or for ventilation and circulation. If the ε_{Nd} signal were a circulation signal, this would require a mixture of 80 ± 10 % AAIW (-6 ± 0.5 ε_{Nd}, *Karas et al.,* 2019) and 20 ± 10 % NADW (between ~- 11.35 and -11.55 ε_{Nd}, *Burton et al.,* 1999). As there is no supporting evidence for such a dramatic increase in the proportion of AAIW from either benthic $\delta^{13}C$ or the carbonate sand percentage (*Haug & Tiedemann,* 1998), we conclude that local inputs of radiogenic terrestrial material dominated the ε_{Nd} signal at Site 999 during the Early Pleistocene.

5. Conclusions

New high-resolution REE and ε_{Nd} records for deep Caribbean ODP Site 999 for the Late Pliocene glacial MIS M2 and the Early Pleistocene glacial-interglacial cycles MIS 95-100 are used to examine whether deep water mass mixing or local terrestrial inputs controlled the Nd isotope record of the deep Caribbean.

The REE compositions recorded by weakly cleaned planktonic foraminifera changed systematically between glacials and interglacials during both investigated time intervals. We find that there was a distinct terrestrial REE signal in the deep Caribbean that was associated with Central American Seaway closure events during the Late Pliocene (MIS M2) and the Early Pleistocene (MIS 100, 98 and 96) linked to sea level low stands and thus enhanced inputs from the shelves. These terrestrial inputs most likely originated from the Magdalena River, albeit with a somewhat more radiogenic composition than today (*Goldstein et al.* 1984). Increased volcanic activity may also have contributed to the REE budget (*Sigurdsson et al., 1997*).

Trends in the Ce/Ce* anomaly appear to be independent from changes in terrestrial inputs and instead indicate that the deep Caribbean was better ventilated during glacial MIS M2 and the later parts of MIS 96, 98 and 100, supporting earlier evidence based on carbonate sand content (*Haug & Tiedemann,* 1998).

Based on the REE compositions and on comparison with other ocean circulation proxies, such as carbonate sand content and benthic $\delta^{13}C$ (*Haug & Tiedemann,* 1998; *De Schepper et al.,* 2013), we find that the ε_{Nd} composition at Site 999 was strongly influenced by local inputs during both time intervals studied. We recommend that studies that aim to use ε_{Nd} as a paleocirculation tracer close to potential inputs from land routinely measure REE compositions to identify any possible terrestrial influence on the signal.

Acknowledgments, Samples, and Data

The data for this paper are available in the supporting information Tables S1–S3 and in the PANGAEA database (https://doi.pangaea.de/10.1594/PANGAEA.907573). This work was funded through German Science Foundation (DFG) project FR1198/8-2 (AO/MF). This research used samples provided by the Ocean Drilling Program (ODP). ODP is sponsored by the U.S.
National Science Foundation (NSF) and participating countries under management of Joint Oceanographic Institutions (JOI), Inc. Chris German and Marcus Gutjahr are thanked for useful discussions. We thank the two reviewers for their constructive comments and Stephen Barker for editorial handling.

References

Abbott, A. N. (2019), A benthic flux from calcareous sediments results in non-conservative neodymium behavior during lateral transport: A study from the Tasman Sea, *Geology*, *47*(4), 363-366.

Abbott, A. N., B. A. Haley, and J. McManus (2015), Bottoms up: Sedimentary control of the deep North Pacific Ocean's epsilon(Nd) signature, *Geology*, *43*(11), 1035-1038.

Abbott, A. N., B. A. Haley, and J. McManus (2016), The impact of sedimentary coatings on the diagenetic Nd flux, *Earth and Planetary Science Letters*, *449*, 217-227.

Abbott, A. N., B. A. Haley, J. McManus, and C. E. Reimers (2015), The sedimentary flux of dissolved rare earth elements to the ocean, *Geochimica Et Cosmochimica Acta*, *154*, 186-200.

Barrat, J. A., F. Keller, J. Amosse, R. N. Taylor, R. W. Nesbitt, and T. Hirata (1996), Determination of rare earth elements in sixteen silicate reference samples by ICP-MS after Tm addition and ion exchange separation, *Geostandards Newsletter*, *20*(1), 133-139.

Bayon, G., C. R. German, K. W. Burton, R. W. Nesbitt, and N. Rogers (2004), Sedimentary Fe-Mn oxyhydroxides as paleoceanographic archives and the role of aeolian flux in regulating oceanic dissolved REE, *Earth and Planetary Science Letters*, *224*(3-4), 477-492.

Blaser, P., J. Lippold, M. Gutjahr, N. Frank, J.M. Link, and M. Frank (2016), Extracting foraminiferal seawater Nd isotope signatures with bulk sediment leaches, *Chemical Geology* 439, 289-304.

Boiteau, R., M. Greaves, and H. Elderfield (2012), Authigenic uranium in foraminiferal coatings: A proxy for ocean redox chemistry, *Paleoceanography*, *27*, PA3227

Boyle, E. A. (1981), Cadmium, zinc, copper, and barium in foramininfera tests, *Earth and Planetary Science Letters*, *53*, 11-35.

Burton, K. W., H. F. Ling, and R. K. Onions (1997), Closure of the Central American Isthmus and its effect on deep-water formation in the North Atlantic, *Nature*, *386*(6623), 382-385.

Burton, K. W., D. C. Lee, J. N. Christensen, A. N. Halliday, and J. R. Hein (1999), Actual timing of neodymium isotopic variations recorded by Fe-Mn crusts in the western North Atlantic, *Earth and Planetary Science Letters*, *171*(1), 149-156.

Byrne, R. H., and K. H. Kim (1990), Rare-earth element scavenging in seawater, *Geochimica Et Cosmochimica Acta*, *54*(10), 2645-2656.

deMenocal, P. B., D. W. Oppo, R. G. Fairbanks, and W. L. Prell (1992), Pleistocene delta C-13 variability of North Atlantic Intermediate Water, *Paleoceanography*, *7*(2), 229-250.

De Schepper, S., J. Groeneveld, B. D. A. Naafs, C. Van Renterghem, J. Hennissen, M. J. Head, S. Louwye, and K. Fabian (2013), Northern Hemisphere Glaciation during the globally warm early Late Pliocene, *PLOS ONE*, *8*(12), e81508.

Dolan, A. M., A. M. Haywood, S. J. Hunter, J. C. Tindall, H. J. Dowsett, D. J. Hill, and S. J. Pickering (2015), Modelling the enigmatic Late Pliocene Glacial Event - Marine Isotope Stage M2, *Global and Planetary Change*, *128*, 47-60.

Du, J. H., B. A. Haley, and A. C. Mix (2016), Neodymium isotopes in authigenic phases, bottom waters and detrital sediments in the Gulf of Alaska and their implications for paleo-circulation reconstruction, *Geochimica Et Cosmochimica Acta*, *193*, 14-35.

Dwyer, G. S., and M. A. Chandler (2009), Mid-Pliocene sea level and continental ice volume based on coupled benthic Mg/Ca palaeotemperatures and oxygen isotopes, *Philosophical Transactions of the Royal Society a-Mathematical Physical and Engineering Sciences*, *367*(1886), 157-168.

Elderfield, H., and M. J. Greaves (1982), The rare-earth elements in seawater, *Nature*, *296*(5854), 214-219.

Elderfield, H., and E. R. Sholkovitz (1987), Rare- earth elements in the pore waters of reducing nearshore sediments, *Earth and Planetary Science Letters*, *82*(3-4), 280-288.

Freslon, N., et al. (2014), Rare earth elements and neodymium isotopes in sedimentary organic matter, *Geochimica Et Cosmochimica Acta*, *140*, 177-198.

Froelich, P. N., G. P. Klinkhammer, M. L. Bender, N. A. Luedtke, G. R. Heath, D. Cullen, P. Dauphin, D. Hammond, B. Hartman, and V. Maynard (1979), Early oxidation of organic matter in pelagic sediments of the eastern equatorial Atlantic - suboxic diagenesis *Geochimica Et Cosmochimica Acta*, *43*(7), 1075-1090.

German, C. R., and H. Elderfield (1990), Application of the Ce anomaly as a paleoredox indicator: the ground rules, *Paleoceanography*, *5*(5), 823-833.

Goldstein, S. L., R. K. Onions, and P. J. Hamilton (1984), A Sm-Nd Isotopic Study of Atmospheric Dusts and Particulates from Major River Systems, *Earth and Planetary Science Letters*, *70*(2), 221-236.

Greaves, M., et al. (2008), Interlaboratory comparison study of calibration standards for foraminiferal Mg/Ca thermometry, *Geochemistry Geophysics Geosystems*, *9*, Q08010.

Grenier, M., C. Jeandel, F. Lacan, D. Vance, C. Venchiarutti, A. Cros, and S. Cravatte (2013), From the subtropics to the central equatorial Pacific Ocean: Neodymium isotopic composition and rare earth element concentration variations, *Journal of Geophysical Research-Oceans*, *118*(2), 592-618.

Groeneveld, J., E. C. Hathorne, S. Steinke, H. DeBey, A. Mackensen, and R. Tiedemann (2014), Glacial induced closure of the Panamanian Gateway during Marine Isotope Stages (MIS) 95-100 (similar to 2.5 Ma), *Earth and Planetary Science Letters*, *404*, 296-306.

Gutjahr, M., M. Frank, C. H. Stirling, L. D. Keigwin, and A. N. Halliday (2008), Tracing the Nd isotope evolution of North Atlantic deep and intermediate waters in the Western North Atlantic since the Last Glacial Maximum from Blake Ridge sediments, *Earth and Planetary Science Letters*, *266*(1-2), 61-77.

Gutjahr, M., M. Frank, C. H. Stirling, V. Klemm, T. van de Flierdt, and A. N. Halliday (2007), Reliable extraction of a deepwater trace metal isotope signal from Fe-Mn oxyhydroxide coatings of marine sediments, *Chemical Geology*, *242*(3-4), 351-370.

Haley, B. A., G. P. Klinkhammer, and J. McManus (2004), Rare earth elements in pore waters of marine sediments, *Geochimica Et Cosmochimica Acta*, *68*(6), 1265-1279.

Haley, B. A., J. H. Du, A. N. Abbott, and J. McManus (2017), The Impact of Benthic Processes on Rare Earth Element and Neodymium Isotope Distributions in the Oceans, *Frontiers in Marine Science*, *4*.

Hathorne, E. C., T. Stichel, B. Bruck, and M. Frank (2015), Rare earth element distribution in the Atlantic sector of the Southern Ocean: The balance between particle scavenging and vertical supply, *Marine Chemistry*, *177*, 157-171.

Hathorne, E. C., B. Haley, T. Stichel, P. Grasse, M. Zieringer, and M. Frank (2012), Online preconcentration ICP-MS analysis of rare earth elements in seawater, *Geochemistry Geophysics Geosystems*, *13*, Q01020.

Haug, G. H., and R. Tiedemann (1998), Effect of the formation of the Isthmus of Panama on Atlantic Ocean thermohaline circulation, *Nature*, *393*(6686), 673-676.

Haug, G. H., K. A. Hughen, D. M. Sigman, L. C. Peterson, and U. Rohl (2001), Southward migration of the intertropical convergence zone through the Holocene, *Science*, *293*(5533), 1304-1308.

Hein, J. R., A. Koschinsky, M. Bau, F. T. Manheim, J.-K. Kang, and L. Roberts (1999), Cobalt-rich ferromanganese crusts in the Pacific, in *Handbook of Marine Mineral Deposits*, edited by D. S. Cronan, pp. 239-279, CRC Press.

Henderson, G. M., and R. K. Onions (1995), U-234/U-238 ratios in Quaternary planktonic foraminifera, *Geochimica Et Cosmochimica Acta*, *59*(22), 4685-4694.

Holser, W. T. (1997), Evaluation of the application of rare-earth elements to paleoceanography, *Palaeogeography Palaeoclimatology Palaeoecology*, *132*(1-4), 309-323.

Huang, K.-F., D. W. Oppo, and W. B. Curry (2014), Decreased influence of Antarctic intermediate wter in the tropical Atlantic during North Atlantic cold events, *Earth and Planetary Science Letters*, *389*, 200-208.

Jacobsen, S. B., and G. J. Wasserburg (1980), Sm-Nd isotopic evolution of chondrites, *Earth and Planetary Science Letters*, *50*(1), 139-155.

James, D. E., and L. A. Murcia (1984), Crustal contamination in northern Andean volcanics, *Journal of the Geological Society*, *141*(SEP), 823-830.

Jeandel, C., D. Thouron, and M. Fieux (1998), Concentrations and isotopic compositions of neodymium in the eastern Indian Ocean and Indonesian straits, *Geochimica Et Cosmochimica Acta*, *62*(15), 2597-2607.

Jeandel, C., T. Arsouze, F. Lacan, P. Techine, and J. C. Dutay (2007), Isotopic Nd compositions and concentrations of the lithogenic inputs into the ocean: A compilation, with an emphasis on the margins, *Chemical Geology*, *239*(1-2), 156-164.

Johns, W. E., T. L. Townsend, D. M. Fratantoni, and W. D. Wilson (2002), On the Atlantic inflow to the Caribbean Sea, *Deep-Sea Research Part I-Oceanographic Research Papers*, *49*(2), 211-243.

Joyce, T. M., R. S. Pickart, and R. C. Millard (1999), Long-term hydrographic changes at 52 and 66 degrees W in the North Atlantic Subtropical Gyre & Caribbean, *Deep-Sea Research Part Ii-Topical Studies in Oceanography*, *46*(1-2), 245-278.

Karas, C., Goldstein, S. L., and deMenocal, P. B. (2019), Evolution of Antarctic Intermediate Water during the Plio-Pleistocene and implications for global climate: Evidence from the South Atlantic, *Quaternary Science Reviews, 221*, 105945.

Kawase, M., and J. L. Sarmiento (1986), Circulation and nutrients in mid-depth Atlantic waters, *Journal of Geophysical Research-Oceans*, *91*(C8), 9749-9770.

Kirillova, V., A. H. Osborne, T. Storling, and M. Frank (2019), Miocene restriction of the Pacific-North Atlantic throughflow strengthened Atlantic overturning circulation, *Nature Communications, 10:4025.*

Koschinsky, A., and J. R. Hein (2003), Uptake of elements from seawater by ferromanganese crusts: solid-phase associations and seawater speciation, *Marine Geology*, *198*(3-4), 331-351.

Kraft, S., M. Frank, E. C. Hathorne, and S. Weldeab (2013), Assessment of seawater Nd isotope signatures extracted from foraminiferal shells and authigenic phases of Gulf of Guinea sediments, *Geochimica Et Cosmochimica Acta*, *121*, 414-435.

Lacan, F., and C. Jeandel (2001), Tracing Papua New Guinea imprint on the central Equatorial Pacific Ocean using neodymium isotopic compositions and Rare Earth Element patterns, *Earth and Planetary Science Letters*, *186*(3-4), 497-512.

Lacan, F., and C. Jeandel (2004a), Subpolar Mode Water formation traced by neodymium isotopic composition, *Geophysical Research Letters*, *31*(14).

Lacan, F., and C. Jeandel (2004b), Neodymium isotopic composition and rare earth element concentrations in the deep and intermediate Nordic Seas: Constraints on the Iceland Scotland Overflow Water signature, *Geochemistry Geophysics Geosystems*, *5*, Q11006.

Lacan, F., and C. Jeandel (2004c), Denmark Strait water circulation traced by heterogeneity in neodymium isotopic compositions, *Deep-Sea Research Part I-Oceanographic Research Papers*, *51*(1), 71-82.

Lacan, F., and C. Jeandel (2005a), Acquisition of the neodymium isotopic composition of the North Atlantic Deep Water, *Geochemistry Geophysics Geosystems*, *6*.

Lacan, F., and C. Jeandel (2005b), Neodymium isotopes as a new tool for quantifying exchange fluxes at the continent-ocean interface, *Earth and Planetary Science Letters*, *232*(3-4), 245-257.

Le Fevre, B., and C. Pin (2005), A straightforward separation scheme for concomitant Lu-Hf and Sm-Nd isotope ratio and isotope dilution analysis, *Analytica Chimica Acta*, *543*(1-2), 209-221.

Lea, D. W., D. K. Pak, and G. Paradis (2005), Influence of volcanic shards on foraminiferal Mg/Ca in a core from the Galapagos region, *Geochemistry Geophysics Geosystems*, *6*, Q11P04.

Lisiecki, L. E., and M. E. Raymo (2005), A Pliocene-Pleistocene stack of 57 globally distributed benthic delta O-18 records, *Paleoceanography*, *20*(1), PA1003.

Lugmair, G. W., T. Shimamura, R. S. Lewis, and E. Anders (1983), Sm-146 in the early solar system - evidence from Neodymium in the Allende meteorite, *Science*, *222*(4627), 1015-1018.

Miller, K. G., M. A. Kominz, J. V. Browning, J. D. Wright, G. S. Mountain, M. E. Katz, P. J. Sugarman, B. S. Cramer, N. Christie-Blick, and S. F. Pekar (2005), The phanerozoic record of global sea-level change, *Science*, *310*(5752), 1293-1298.

Naish, T., et al. (2009), Obliquity-paced Pliocene West Antarctic ice sheet oscillations, *Nature*, *458*(7236), 322-U384.

Naish, T. R., and G. S. Wilson (2009), Constraints on the amplitude of Mid-Pliocene (3.6-2.4 Ma) eustatic sea-level fluctuations from the New Zealand shallow-marine sediment record, *Philosophical Transactions of the Royal Society a-Mathematical Physical and Engineering Sciences*, *367*(1886), 169-187.

Nie, J. S., B. K. Horton, J. E. Saylor, A. Mora, M. Mange, C. N. Garzione, A. Basu, C. J. Moreno, V. Caballero, and M. Parra (2012), Integrated provenance analysis of a convergent retroarc foreland system: U-Pb ages, heavy minerals, Nd isotopes, and sandstone compositions of the Middle Magdalena Valley basin, northern Andes, Colombia, *Earth-Science Reviews*, *110*(1-4), 111-126.

Osborne, A. H., D. R. Newkirk, J. Groeneveld, E. E. Martin, R. Tiedemann, and M. Frank (2014a), The seawater neodymium and lead isotope record of the final stages of Central American Seaway closure, *Paleoceanography*, *29*(7), 715-729.

Osborne, A. H., B. Haley, E. C. Hathorne, S. Flögel, and M. Frank (2014b), Neodymium isotopes and concentrations in Caribbean seawater: Tracing water mass mixing and

continental unput in a semi-enclosed ocean basin, *Earth and Planetary Science Letters*, *406*, 174-186.
Osborne, A. H., B. A. Haley, E. C. Hathorne, Y. Plancherel, and M. Frank (2015), Rare earth element distribution in Caribbean seawater: Continental inputs versus lateral transport of distinct REE compositions in subsurface water masses, *Marine Chemistry*, *177*, 172-183.
Osborne, A. H., E. C. Hathorne, J. Schijf, Y. Plancherel, P. Boning, and M. Frank (2017), The potential of sedimentary foraminiferal rare earth element patterns to trace water masses in the past, *Geochemistry Geophysics Geosystems*, *18*(4), 1550-1568.
Piepgras, D. J., and G. J. Wasserburg (1987), Rare-Earth Element Transport in the Western North-Atlantic Inferred from Nd Isotopic Observations, *Geochimica Et Cosmochimica Acta*, *51*(5), 1257-1271.
Piotrowski, A. M., A. Galy, J. A. L. Nicholl, N. Roberts, D. J. Wilson, J. A. Clegg, and J. Yu (2012), Reconstructing deglacial North and South Atlantic deep water sourcing using foraminiferal Nd isotopes, *Earth and Planetary Science Letters*, *357*, 289-297.
Pourmand, A., J. M. Prospero, and A. Sharifi (2014), Geochemical fingerprinting of trans-Atlantic African dust based on radiogenic Sr-Nd-Hf isotopes and rare earth element anomalies, *Geology*, *42*(8), 675-678.
Quandt, D., et al. (2018), The geochemistry and geochronology of Early Jurassic igneous rocks from the Sierra Nevada de Santa Marta, NW Colombia, and tectono-magmatic implications, *Journal of South American Earth Sciences*, *86*, 216-230.
Restrepo, J. D., P. Zapata, J. A. Diaz, J. Garzon-Ferreira, and C. B. Garcia (2006), Fluvial fluxes into the Caribbean Sea and their impact on coastal ecosystems: The Magdalena River, Colombia, *Global and Planetary Change*, *50*(1-2), 33-49.
Rincon-Martinez, D., F. Lamy, S. Contreras, G. Leduc, E. Bard, C. Saukel, T. Blanz, A. Mackensen, and R. Tiedemann (2010), More humid interglacials in Ecuador during the past 500 kyr linked to latitudinal shifts of the equatorial front and the Intertropical Convergence Zone in the eastern tropical Pacific, *Paleoceanography*, *25*,PA2210.
Roberts, N. L., A. M. Piotrowski, J. F. McManus, and L. D. Keigwin (2010), Synchronous Deglacial Overturning and Water Mass Source Changes, *Science*, *327*(5961), 75-78.
Roberts, N. L., A. M. Piotrowski, H. Elderfield, T. I. Eglinton, and M. W. Lomas (2012), Rare earth element association with foraminifera, *Geochimica Et Cosmochimica Acta*, *94*, 57-71.
Rohling, E. J., G. L. Foster, K. M. Grant, G. Marino, A. P. Roberts, M. E. Tamisiea, and F. Williams (2014), Sea-level and deep-sea-temperature variability over the past 5.3 million years (vol 508, pg 477, 2014), *Nature*, *510*(7505), 432-432.
Rosenthal, Y., M. P. Field, and R. M. Sherrell (1999), Precise determination of element/calcium ratios in calcareous samples using sector field inductively coupled plasma mass spectrometry, *Analytical Chemistry*, *71*(15), 3248-3253.
Scher, H. D., and E. E. Martin (2006), Timing and climatic consequences of the opening of Drake Passage, *Science*, *312*(5772), 428-430.
Schijf, J., E. A. Christenson, and R. H. Byrne (2015), YREE scavenging in seawater: A new look at an old model, *Marine Chemistry*, *177*, 460-471.
Schlitzer, R. (2018), Ocean Data View, http://odv.awi.de/.
Sholkovitz, E. R. (1993), The geochemistry of rare-earth elements in the Amazon River estuary, *Geochimica Et Cosmochimica Acta*, *57*(10), 2181-2190.
Sholkovitz, E. R., T. J. Shaw, and D. L. Schneider (1992), The geochemistry of rare-earth elements in the seasonally anoxic water column and porewaters of Chesapeake Bay, *Geochimica Et Cosmochimica Acta*, *56*(9), 3389-3402.

Sigurdsson, H., R. M. Leckie, G. D. Acton, and S. S. Party (1997), Site 999, *Proceedings of the Ocean Drilling Program, Initial Reports, 202*, 131-230.

Skinner, L. C., A. Sadekov, M. Brandon, M. Greaves, Y. Plancherel, M. de la Fuente, J. Gottschalk, S. Souanef-Ureta, S. Sevilgen, and A. E. Scrivner (2019), Rare Earth Elements in early-diagenetic foraminifer 'coatings': Pore-water controls and potential palaeoceanographic applications, *Geochimica Et Cosmochimica Acta*, *245*, 118-132.

Steph, S., R. Tiedemann, M. Prange, J. Groeneveld, D. Nurnberg, L. Reuning, M. Schulz, and G. H. Haug (2006), Changes in Caribbean surface hydrography during the Pliocene shoaling of the Central American Seaway, *Paleoceanography*, *21*(4), PA4221.

Stewart, J. A., M. Gutjahr, R. H. James, P. Anand, and P. A. Wilson (2016), Influence of the Amazon River on the Nd isotope composition of deep water in the western equatorial Atlantic during the Oligocene-Miocene transition, *Earth and Planetary Science Letters*, *454*, 132-141.

Tachikawa, K., A. M. Piotrowski, and G. Bayon (2014), Neodymium associated with foraminiferal carbonate as a recorder of seawater isotopic signatures, *Quaternary Science Reviews*, *88*, 1-13.

Tachikawa, K., M. Roy-Barman, A. Michard, D. Thouron, D. Yeghicheyan, and C. Jeandel (2004), Neodymium isotopes in the Mediterranean Sea: Comparison between seawater and sediment signals, *Geochimica Et Cosmochimica Acta*, *68*(14), 3095-3106.

Tanaka, T., et al. (2000), JNdi-1: a neodymium isotopic reference in consistency with LaJolla neodymium, *Chemical Geology*, *168*(3-4), 279-281.

Taylor, S. R., and S. M. McLennan (1985), *The Continental Crust: Its Composition and Evolution.* Blackwell Scientific Publications, Oxford.

Wilson, D. J., A. M. Piotrowski, A. Galy, and I. N. McCave (2012), A boundary exchange influence on deglacial neodymium isotope records from the deep western Indian Ocean, *Earth and Planetary Science Letters*, *341*, 35-47.

Wüst, G. (1964), *Stratification and Circulation in the Antillean-Caribbean Basins, Part 1, Spreading and mixing of the water types with an oceanographic atlas*, 201 pp., Columbia University Press, New York.

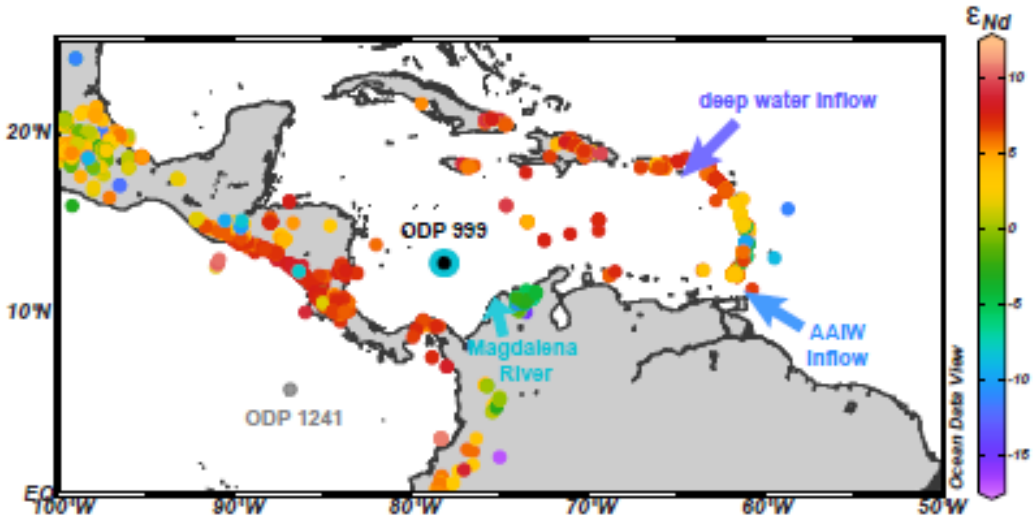

Figure 1. Map showing the locations of cores discussed in the text and ε_{Nd} compositions of rock samples from the Caribbean region (small coloured circles), as retrieved from the GEOROC database (http://georoc.mpch-mainz.gwdg.de/georoc/). Also shown is the ε_{Nd} composition calculated for the deepest waters entering the Caribbean basin via the Anegada-Jungfern sill at ~ 1800 m (~ -13 ε_{Nd}, *deMenocal et al.,* 1992; *Kawase & Sarmiento,* 1986; *Piepgras & Wasserburg*, 1987; *Tachikawa et al.,* 2004), the ε_{Nd} composition of AAIW transported from the South Atlantic (-10.6 to -11 ε_{Nd}, *Osborne et al.,* 2014b) and the ε_{Nd} composition of Magdalena River sediments (ε_{Nd} = -8.3, *Goldstein et al.,* 1984). The coloured circle around Site 999 shows the composition of present day Caribbean seawater at 3000 m depth from a station close to ODP Site 999 (*Osborne et al.,* 2014b). Map produced using Ocean Data View (*Schlitzer*, 2018).

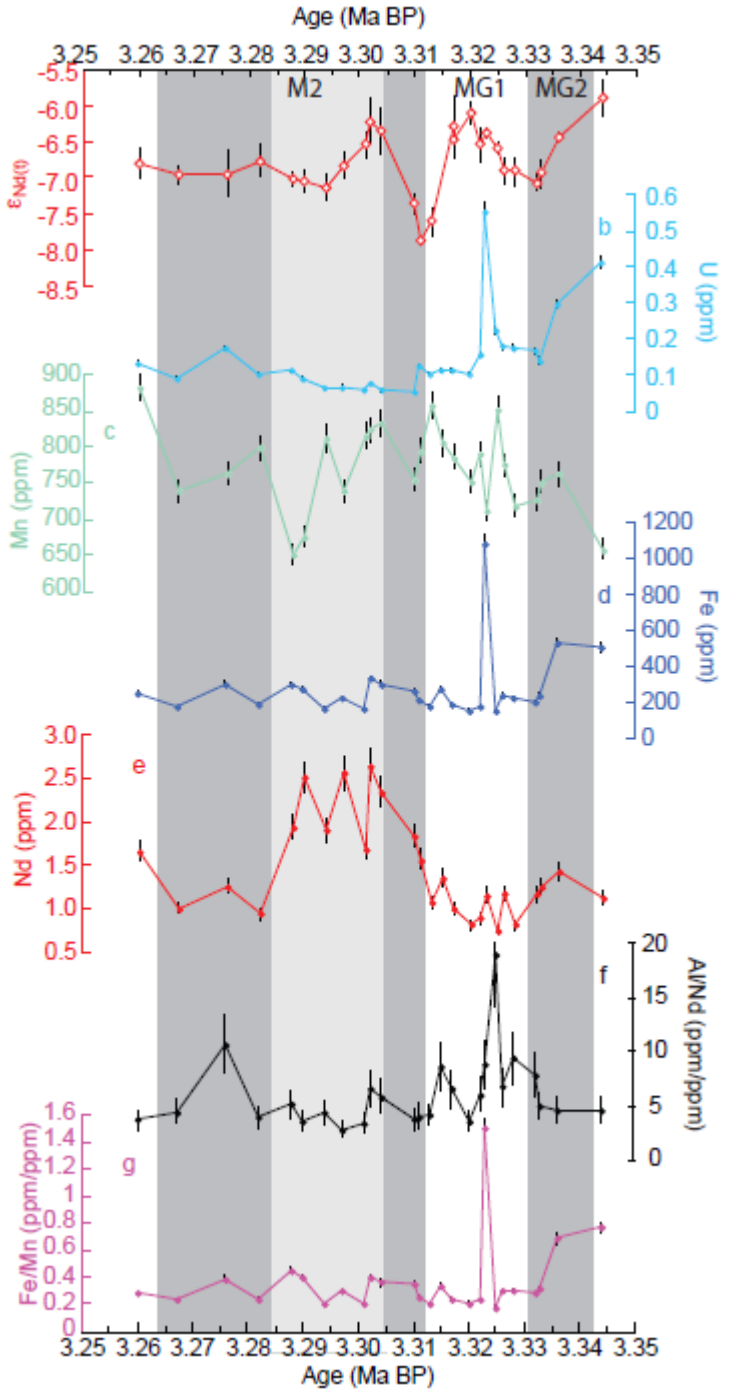

Figure 2. High-resolution data from weakly cleaned foraminifera for MIS M2 at ODP Site 999: (a) ε_{Nd}; (b) U (ppm); (c) Mn (ppm); (d) Fe (ppm); (e) Nd (ppm); (f) Al/Nd (ppm/ppm); (g) Fe/Mn (ppm/ppm). The dark grey vertical bars indicate the extent of the glacials MIS MG2 and M2, based on benthic $\delta^{18}O$ (*Lisiecki & Raymo, 2005*) and the lighter grey vertical bar indicates the extent of the most intense glaciation during M2, from 3.305 -3.285 Ma (*De Schepper et al.,* 2013).

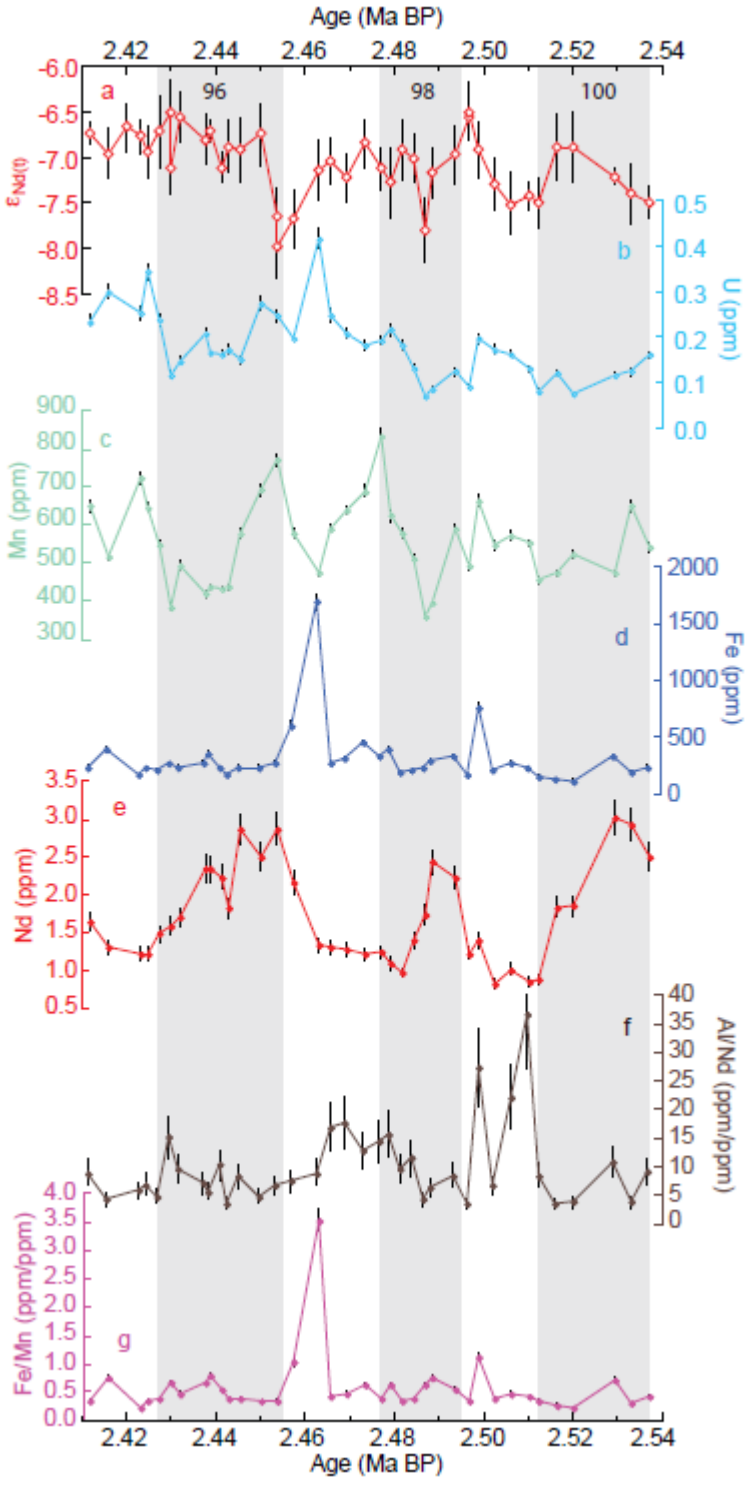

Figure 3. High-resolution data from weakly cleaned foraminifera for MIS 95-100 at ODP Site 999: (a) ε_{Nd}; (b) U (ppm); (c) Mn (ppm); (d) Fe (ppm); (e) Nd (ppm); (f) Al/Nd (ppm/ppm); (g) Fe/Mn (ppm/ppm). The light grey vertical bars indicate the extent of the glacials MIS 96, 98 and 100, based on benthic $\delta^{18}O$ (*Lisiecki & Raymo, 2005*).

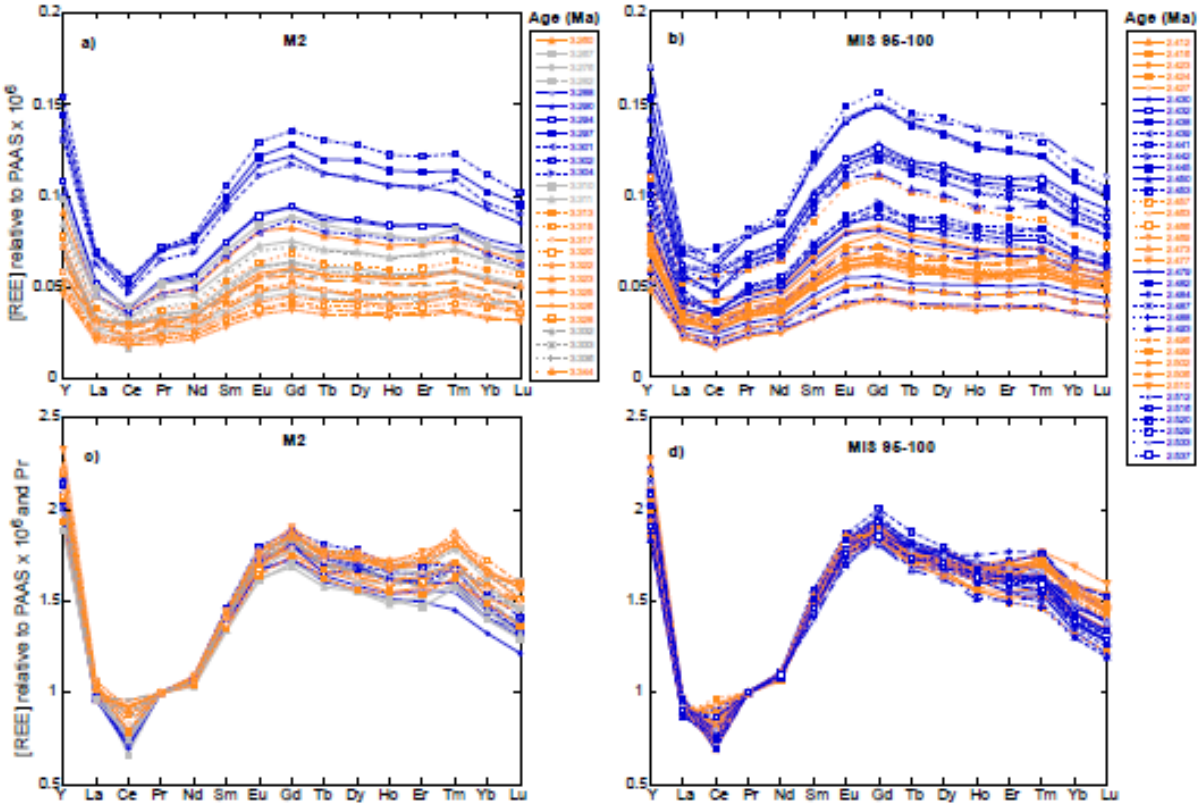

Figure 4 YREE concentrations measured in weakly cleaned foraminifera normalized to Post Archean Australian Shale values (PAAS, *Taylor & McLennan,* 1985) for (a) M2 and (b) MIS 95-100. The PAAS-normalized YREE values were further normalized to [Pr] in figures (c) and (d) to better compare the shapes of the YREE patterns. Orange symbols in all plots indicate interglacial samples. Blue symbols in plots (a) and (c) indicate samples from the most intense glaciation during M2, from 3.305 -3.285 Ma (*De Schepper et al.,* 2013), whereas grey symbols in plots (a) and (c) indicate other glacial samples. Blue symbols in plots (b) and (d) indicate glacial samples.

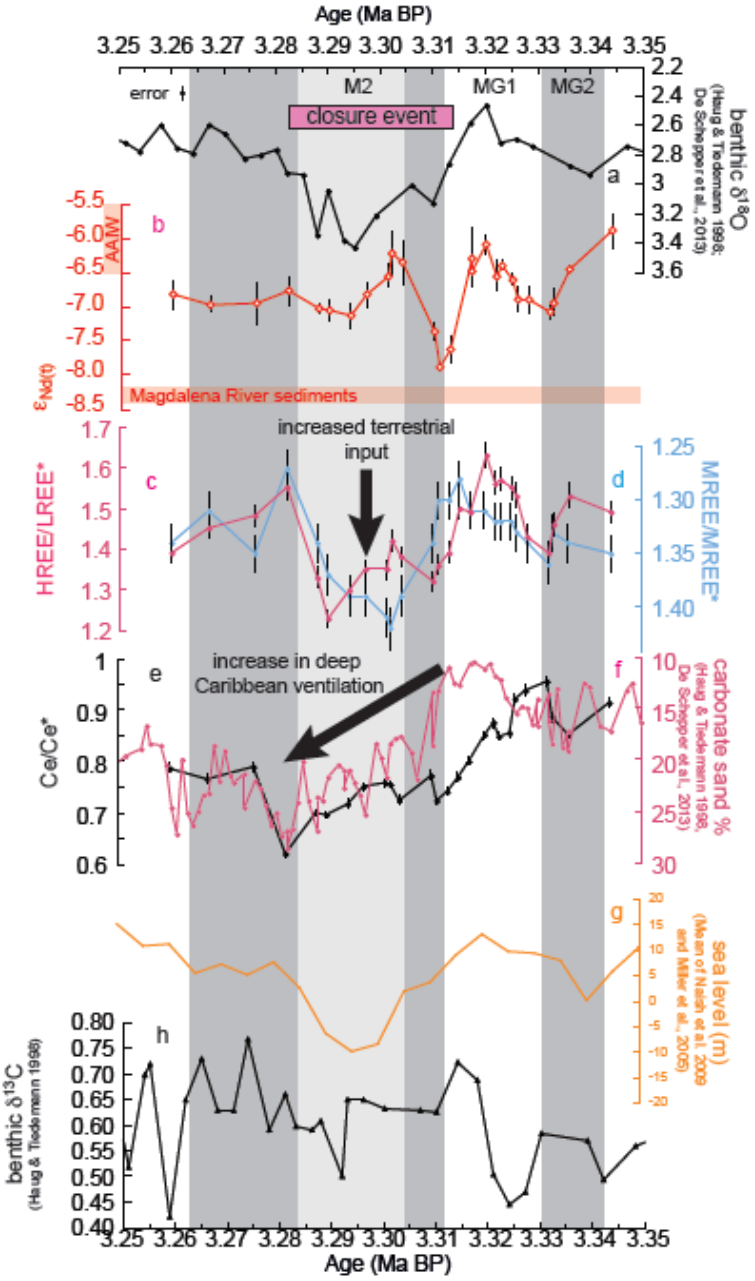

Figure 5. High-resolution data for MIS M2 from ODP Site 999: (a) benthic foraminifer $\delta^{18}O$ (*Haug & Tiedemann*, 1998; *De Schepper et al.,* 2013), (b) ε_{Nd}, (c) HREE/LREE, (d) MREE/MREE*, and (e) Ce/Ce* in weakly cleaned foraminifera; (f) carbonate sand percentage (*Haug & Tiedemann*, 1998; *De Schepper et al.,* 2013), (g) mean of sea level estimates from *Naish et al.* (2009) and *Miller et al.* (2005), scaled to the amplitudes of the *Lisiecki & Raymo,* (2005) benthic foraminifer $\delta^{18}O$ record , as calculated by *Rohling et al.* (2014), and (h) benthic foraminifer $\delta^{13}C$ (*Haug & Tiedemann*, 1998). Also shown is a pink horizontal bar indicating the extent of a sea-level driven Central American Seaway closure event, based on dinoflagellate assemblages (*De Schepper et al.,* 2013). The horizontal red bar in plot (b) shows the composition of Magdalena River sediments (*Goldstein et al.,* 1984). The vertical red bar in plot (b) shows the composition of AAIW during this time interval (*Karas et al.,* 2019). The dark grey vertical bars indicate the duration of the MIS MG2 and M2 glacials, based on benthic foraminiferal $\delta^{18}O$ (*Lisiecki & Raymo, 2005*) and the lighter grey vertical bar indicates the extent of the most intense glaciation during MIS M2, from 3.305 -3.285 Ma (*De Schepper et al.,* 2013).

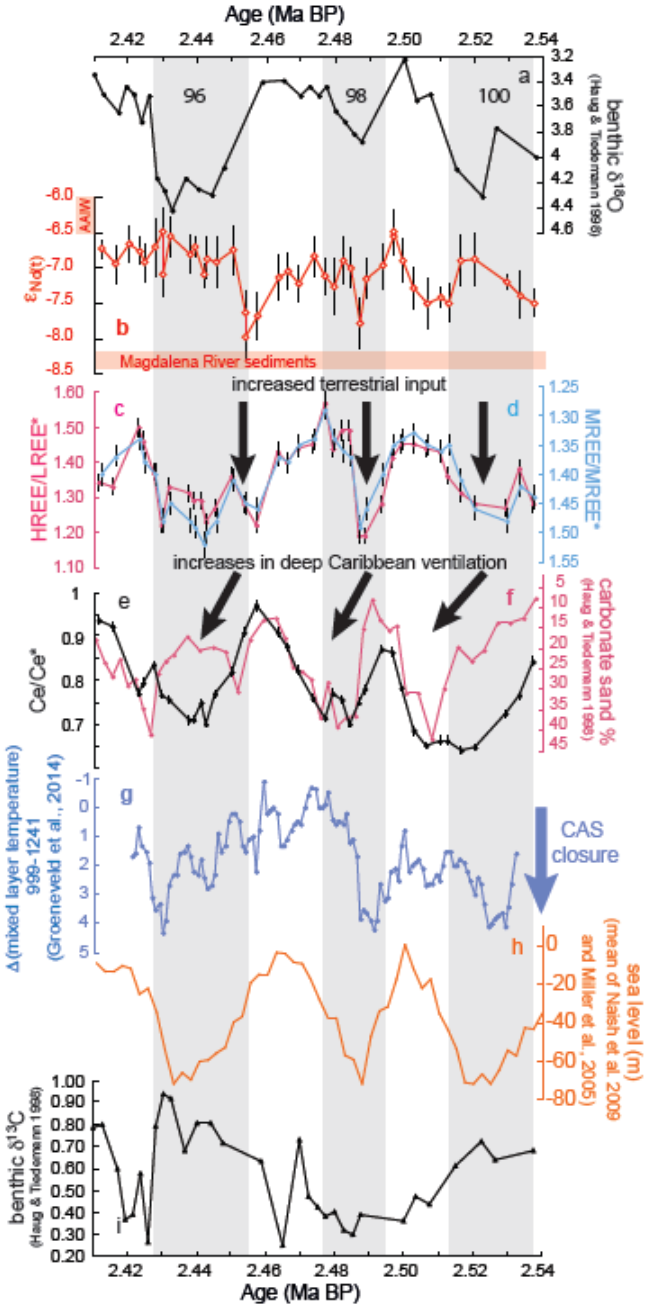

Figure 6. High-resolution data for MIS 95-100 from ODP Site 999: (a) benthic foraminifer $\delta^{18}O$ (*Haug & Tiedemann*, 1998), (b) ε_{Nd}, (c) HREE/LREE, (d) MREE/MREE*, and (e) Ce/Ce* in weakly cleaned foraminifera; (f) carbonate sand percentage (*Haug & Tiedemann*, 1998), (g) Caribbean-Pacific difference in mixed layer temperature (*Groeneveld et al.,* 2014), (h) mean of sea level estimates from *Naish et al.* (2009) and *Miller et al.* (2005), scaled to the amplitudes of the *Lisiecki & Raymo,* (2005) benthic foraminifer $\delta^{18}O$ record , as calculated by *Rohling et al.* (2014), (i) benthic foraminifer $\delta^{13}C$ (*Haug & Tiedemann*). The horizontal red bar in plot (b) shows the composition of Magdalena River sediments (*Goldstein et al.,* 1984). The vertical red bar in plot (b) shows the composition of AAIW during this time interval (*Karas et al.,* 2019). The blue arrow in plot (g) indicates increasing differences in Caribbean-Pacific mixed layer temperature, interpreted as resulting from episodic closure of the CAS (*Groeneveld et al.,* 2014). The light grey vertical bars indicate the duration of the glacials MIS 96, 98 and 100, based on benthic foraminiferal $\delta^{18}O$ (*Lisiecki & Raymo, 2005*).